



Optimization of Hydrogen Production by Ethanol Steam Reforming Using Maximization of H₂/CO Ratio with Taguchi Experimental Design Method

¹Ali Reza Karimzadeh, ²Hamid Modarress and ³Ali Eliassi

¹Department of Chemistry, Amirkabir University of Technology, Tehran, Iran

²Department of Chemical Engineering, Amirkabir University of Technology, Tehran, Iran

³Chemical Technologies Research Department,
Iranian Research Organization for Science and Technology (IROST), Tehran, Iran

(Received: August 10, 2012; Accepted in Revised Form: February 12, 2013)

Abstract: In this study the effects of some different factors on ceria (CeO₂) catalytic activity for ethanol steam reforming (ESR) to produce high H₂/CO ratio were investigated. The considered factors were sonication time in three durations (0, 15 and 30 minutes), calcination temperature at three temperatures (500, 650 and 800°C), mole ratio of H₂O/ethanol in three ratios (3, 5 and 8) and reactor temperature at three temperatures (300, 350 and 400°C). The Taguchi L₉ experimental design method was used to investigate the effect of these parameters on maximization of H₂/CO. To identify the catalyst characteristics XRD, SEM, EDS, BET and TGA analysis were done. It was established that a face centered cubic crystal forms of nano particles of CeO₂ were formed. Also the obtained results showed that by increasing calcination temperature or reducing the sonication time, the nano particle size was increased. The reactor tests showed that the optimum conditions for maximization of H₂/CO ratio were: sonication time zero, calcination temperature 800°C, H₂O/ethanol ratio 3 and reactor temperature 300°C. The mole percent of H₂ and CO in these conditions were 64.46 and 0.011%, respectively.

Key words: Hydrogen · Ceria · Ethanol · Taguchi

INTRODUCTION

Hydrogen is expected to become an alternative fuel and a significant source of clean energy via fuel cell systems in the near, medium- and long-term future. Until much progress is made in this field, sources of hydrogen may be found in many various processes utilizing a variety of raw materials [1].

For stationary big users or those within the range of the distribution network, hydrogen will probably be obtained from natural gas or from coal gasification. For some mobile users and, mainly for small stationary but scattered users having no access to hydrogen distribution network, a good solution seems to be the conversion of liquid fuels, such as alcohols or hydrocarbons, realized directly in the site of hydrogen use [2].

Among the various processes used to obtain hydrogen, the steam reforming of natural gas and methanol are custom. But, ethanol steam reforming (ESR) is an interesting alternative, because this alcohol can be a renewable raw material, which can easily be derived from biomass and the carbon dioxide produced in the reforming process is then consumed in biomass growth, thus completing a nearly closed carbon cycle. Moreover, ethanol has other advantages, such as low toxicity, storage and a handling safety and relatively high hydrogen content [3]. ESR can be described by the following equation:



ESR comprises several catalytic steps, which depend on the catalytic systems and reactor conditions [4–16]. Such reaction pathways include dehydration,

Table 1: Experimental conditions for the preparation of ceria

Sample	Sonication time (min)	Calcination temperature (°C)	Time of calcinations (h)
0	-	-	-
1	0	500	1
2	0	650	1
3	0	800	1
4	15	500	1
5	15	650	1
6	15	800	1
7	30	500	1
8	30	650	1
9	30	800	1

decomposition and dehydrogenation of ethanol to form ethylene, methane (or acetone) and acetaldehyde, respectively, besides the water-gas shift reaction (WGS) and methanation reaction [17].

In a number of different studies, various metal catalysts such as: Ni [4], Co [5,6], Ni-Cu [7], Pt, Pd, Rh [8-10] supported on metal oxides (Al_2O_3 , La_2O_3 , ZnO , MgO and etc. [11]) have proved to be suitable for the ethanol steam reforming reaction.

The thermodynamic aspects of the ethanol steam reforming system have received great attention among researchers working in this area. Operating conditions such as temperature, pressure, water-to-ethanol molar ratio and residence time have been optimized to maximize hydrogen production.

The aim of this study is to optimize a catalytic system based on CeO_2 and reactor conditions for steam reforming of ethanol to produce hydrogen with maximum amount of H_2 to CO ratio for polymeric fuel cells applications. CeO_2 has the ability to promote CO oxidation and water-gas shift reaction [13]. The Taguchi L_9 experimental design method was used to investigate the effect of some different parameters such as: sonication time, calcination temperature, mole ratio of H_2O /ethanol and reactor temperature, on maximization of H_2 to CO ratio.

Experimental: CeO_2 nanoparticles was prepared by a precipitation method using $\text{Ce}(\text{NO}_3)_3 \cdot 6\text{H}_2\text{O}$ (Merck, purity >98.5%) and triethylamine (TEA, Merck, purity >99%). Initially, $\text{Ce}(\text{NO}_3)_3 \cdot 6\text{H}_2\text{O}$, 4.342 g (0.01 mol) was dissolved in 100 ml distilled water. The TEA was then added drop wise to the cerium nitrate hexahydrate solution under constant stirring using a magnetic stirrer. The aqueous clear solutions turned yellowish white initially but as the reaction proceeded, it converted into light yellow colloidal suspension. The reaction was allowed to proceed for 1 hr after the complete addition of TEA under stirring at room temperature. The addition time of TEA was about 5 min. The resultant synthesis gel was

then washed thrice with distilled water and dried at 110°C for 4 hr. Dried gel was added to ethanol (Merck, Germany, purity >96%) and was ultrasonically irradiated in different times (0, 15 and 30 min) with a high density ultrasonic probe (Sonicator Hielscher, UP200S, Germany) immersed directly into the solution. The resulted products were collected by centrifugation at 6000 rpm and was washed with ethanol solution and dried in room temperature for 48 hr and then was calcined at different temperatures (500, 650 and 800°C) for 1hr. Experimental conditions for preparation of different samples of ceria, such as sonication time, calcination temperatures and time of calcinations are reported in Table 1.

The obtained powders were characterized by X-ray diffraction (XRD) using a (Inel, EQUINOX 3000, France) with $\text{Cu-K}\alpha$ radiation ($\lambda=1.5406 \text{ \AA}$) in the 2θ range from 10 to 80° with $0.02^\circ/\text{min}$. The crystallites size was calculated using the Scherrer equation [18], from the most intense reflections observed for the CeO_2 crystallographic faces: (111), (220), (311). Thermogravimetric analysis (TGA) studies of the dried gel were performed using Thermal Analyser (Netzsch, TG 209F1 Iris, Germany) between 25 and 900°C . The sample was heated in N_2 atmosphere in alumina crucible at the rate of 10 K/min . Sample preparation for Scanning Electron Microscopy (SEM) includes the deposition of gold on CeO_2 powder. SEM of the samples was carried out on a Seron Technology AIS2100 (Korea), to estimate the surface characteristics of the sample. This instrument was equipped with an energy dispersive X-ray spectrometer. The BET surface area of samples were measured by the low temperature (77 K) nitrogen adsorption in the NOVA 1000 (Quantochrom) analyser, assuming that one nitrogen molecule occupies the area of 0.162 nm^2 .

The reforming reaction was conducted in a stainless steel fixed-bed reactor with inner diameter 19 mm at atmospheric pressure. A thermocouple was located inside the reactor tube, near of the catalyst bed. For each experiment 1 g of the catalyst was used. After this step, the ethanol and water mixture was pumped into the reactor at a flow rate of $30 \text{ cm}^3 \text{ h}^{-1}$. Before entering the feed in to the reactor, the mixture was preheated up to 150°C . The gases at the outlet of the reactor were taken out intermittently with the aid of a sampler directly connected to the system and analyzed on-line by gas chromatography (Teif Gostar, Iran) with a TCD and a packed column (Molecular Sieve 5A). Reaction data were reported after about 4 h when the steady state conditions were obtained for each temperature. A schematic view of the experimental setup is shown in Figure 1.

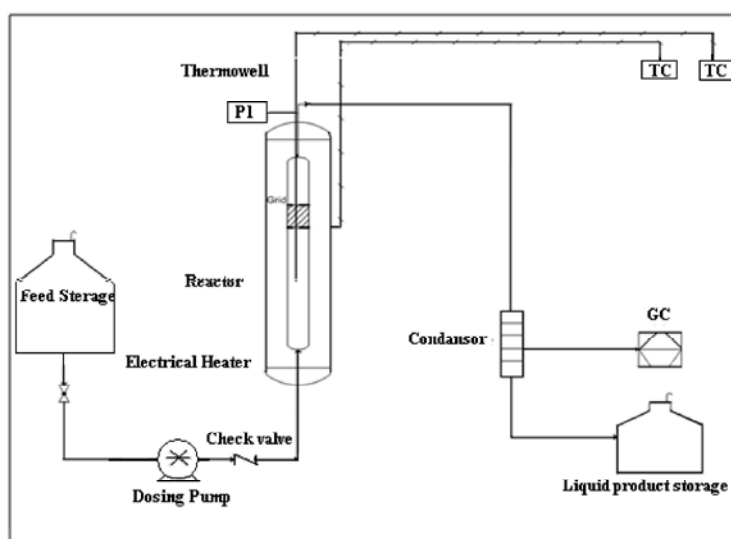


Fig. 1: Schematic view of the experimental setup

As a result of the products variation, the catalyst performance was characterized by two parameters. S_i represents the product distribution percent of component i . Ethanol conversion percent denoted as X_{EtOH} . They were calculated according to Eqs. (2) and (3):

$$X_{EtOH} = \frac{\text{mol EtOH}_{in} - \text{mol EtOH}_{out}}{\text{mol EtOH}_{in}} 100 \quad (2)$$

$$S_i = \frac{P_i}{\sum_{i=1}^n P_i} 100 \quad (3)$$

Where, P_i is the molar amount of product i .

The considered factors were the sonication time in three durations (0, 15 and 30 minutes), calcination temperature at three temperatures (500, 650 and 800°C), mole ratio of H₂O/ethanol in three ratios (3, 5 and 8) and reactor temperature at three temperatures (300, 350 and 400°C). For design of experiments with four factors and three levels for each factor, the fractional factorial design, i.e. a standard L₉ orthogonal array [19] was employed. Each row of the matrix represents one run. However, the sequence in which these runs are carried out is randomized. The three levels of each factor are represented by a "1" or a "2" or a "3" in the matrix. The factors and their levels are assigned in Table 2. Table 3 shows the standard L₉ orthogonal array. Factors A, B, C and D are arranged in column 1, 2, 3 and 4, respectively. For analysis of the results and optimization of conditions for setting the control factors, QUALITEK-4 software was used.

Table 2: Factors and their levels for design of experiments

Factor	Level		
	1	2	3
(A) Sonication time (min)	0	15	30
(B) Calcination temperature (°C)	500	650	800
(C) H ₂ O/EtOH	3	5	8
(D) Reactor temperature (°C)	300	350	400

Table 3: L₉ orthogonal arrays

Experiment no.	Factor levels			
	A	B	C	D
1	1	1	1	1
2	1	2	2	2
3	1	3	3	3
4	2	1	2	3
5	2	2	3	1
6	2	3	1	2
7	3	1	3	2
8	3	2	1	3
9	3	3	2	1

RESULTS AND DISCUSSIONS

Catalyst Characterization: X-ray diffraction is a versatile, non-destructive analytical method for identification and quantitative determination of various crystalline forms, known as 'phases' of compound present in powder and solid samples. Diffraction occurs as waves interact with a regular precipitated solid matrix structure whose repeat distance is about the same as the wavelength. For the samples, the XRD pattern (Figure 2) shows seven reflections (111), (200), (220), (311), (222), (400) and (331)

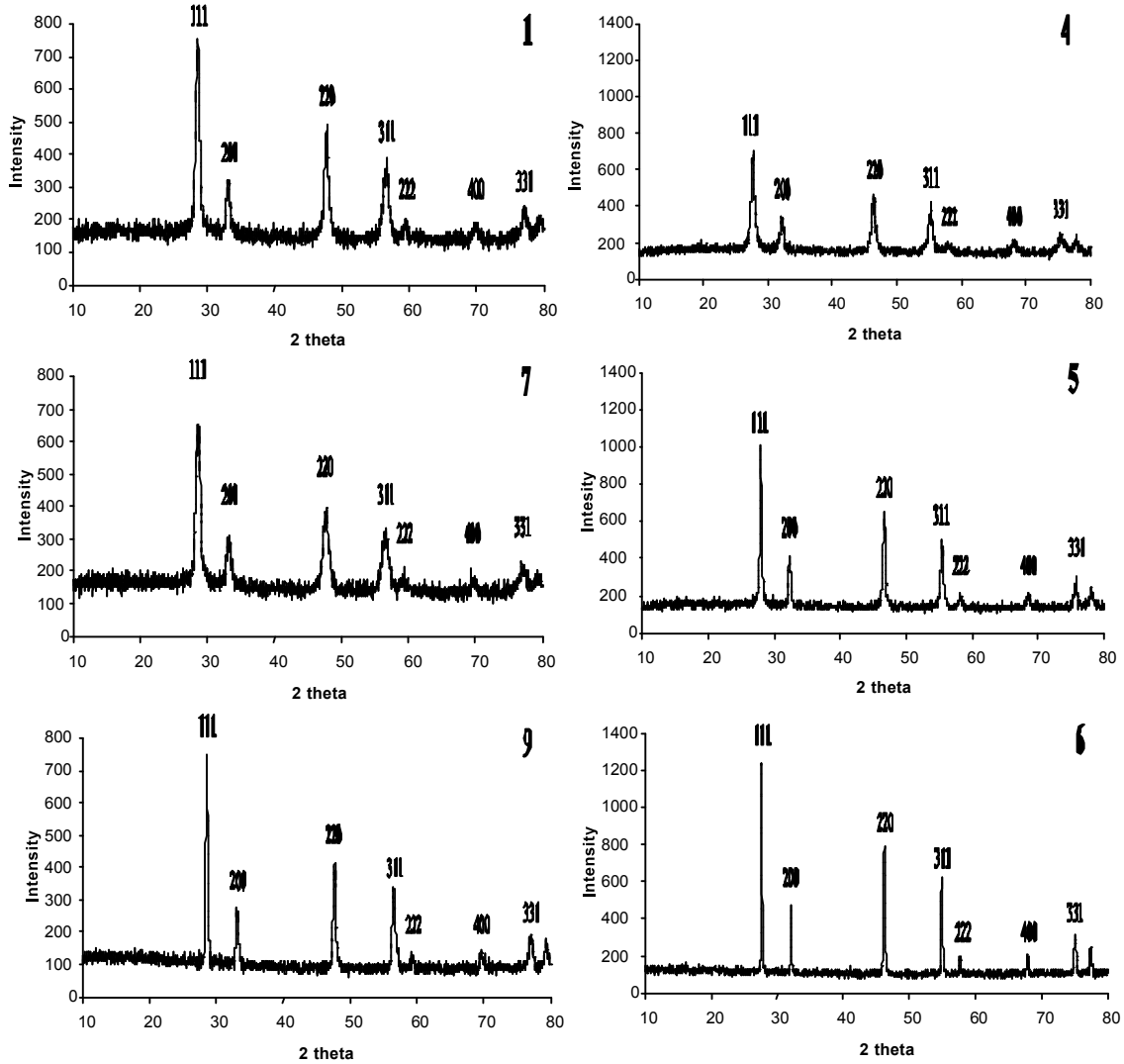


Fig. 2: XRD patterns of samples 1, 4, 5, 6, 7 and 9.

which are characteristics of CeO₂ cubic phase with face centered (Fluorite) structure (Ref. JCPDS card 34-394) [20]. Crystallite size of the metal oxide samples may be obtained using the Scherrer equation. The Scherrer equation is used frequently in X-ray analysis of materials, particularly powder diffraction of metal oxides [21]. It relates the peak breadth of a specific phase of a material to the mean crystallite size of that material. From the full width at half-maximum (FWHM) of the diffraction peaks, the average size of the particles (crystallite) can be estimated from the Scherrer equation. The crystallite size of CeO₂ was estimated from the XRD line widths obtained for faces (hkl) of (111), (220) and (311). The lattice parameter (*a*) was calculated by the following well known Eq. (4):

$$a = \frac{d}{\sqrt{h^2 + k^2 + l^2}} \quad (4)$$

where '*a*' refers to the CeO₂ FCC lattice parameter and *h*, *k*, *l* are the crystalline face Miller indexes and '*d*' is the crystalline face spacing [22]. The unit cell volumes calculated for the ceria particles remained uniform for different samples. The theoretical density, *T_d* is calculated using the Eq. 5 [23]:

$$T_d = \frac{ZMc}{V_c N_A} \quad (5)$$

Table 4: XRD data obtained on CeO₂ powder

Sample no.	<i>d</i> (Å, from 2θ~28°)	Unit Cell parameter 'a' (Å)	Unit cell volume (Å ³)	Crystallite size (nm)	Theoretical density (g/cc)
JCPDS 34-394	3.111	5.389	156.5	-	7.303
1	3.102	5.373	155.1	15.4	7.369
4	3.167	5.485	165.0	21.5	6.927
5	3.142	5.442	161.2	30.1	7.090
6	3.172	5.494	165.8	44.7	6.893
7	3.099	5.368	154.7	11.5	7.388
9	3.105	5.378	155.5	26.5	7.350

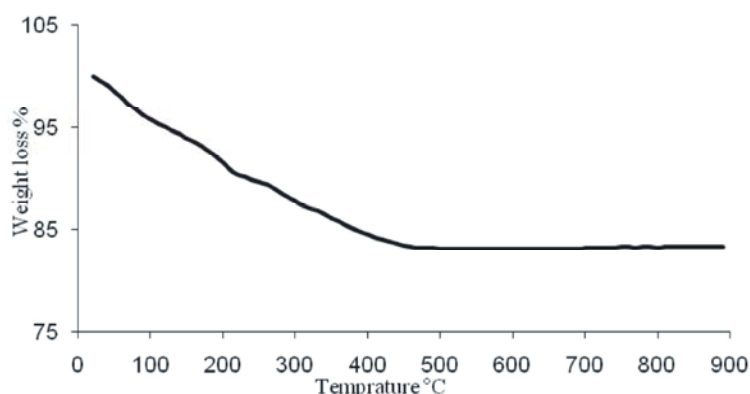


Fig. 3: TGA graph of the sample 0

where 'Z' is the number of chemical species in the unit cell, 'Mc' is the molar mass of a single chemical species corresponding to the chemical formula (gmol^{-1}), 'Vc' is the unit cell volume (\AA^3) and 'N_A' is Avogadro's number ($6.022 \times 10^{23} \text{ mol}^{-1}$). The results are reported in the Table 4.

The results reveal that the size of CeO₂ nanoparticles depends on the calcination temperature. By increasing calcinations temperature, the larger CeO₂ particles have been prepared also crystallinity are increased. By decreasing the sonication time, the broadening of CeO₂ peaks decreases which shows growing of the CeO₂ nanocrystals.

The thermogravimetric (TGA) analysis (Figure 3) show the weight loss of synthesized CeO₂ sample. It has been observed that continuous weight loss was occurred for sample 0. As it can be seen, the rate of weight loss is very high up to 230°C which is attributed to evaporation of absorbed water and dehydration of the dried gel. With removing the water and hydroxyl groups the rate of weight loss decreases with increasing the temperature. The weight loss after 230°C is due to the remaining volatile components, such as nitrate components and CeO₂ formation. The total weight loss of 16.5% appears in the gel after heat treatment at 900°C. No significant weight loss occurs after 470°C that shows all volatile components has left the gel after this temperature.

For investigating the effect of sonication time on the particle size of the ceria, the reactions were carried out at 0, 15 and 30 min (The powders heat treated at 650°C). The SEM micrographs (Figures 4 and 5) of the samples 2, 5 and 8 support the obtained results from the XRD patterns. Comparison of the SEM images results of CeO₂ samples at the SEM magnification of 5000 and 20000X indicates that an increasing the sonication time the synthesized CeO₂ shows not only comparatively smaller particle size but also considerably less agglomeration. Here, we have interestingly observed that the structure of sample 2 consists of small particles aggregated with larger particles but this is not observed for samples 5 and 8.

The energy dispersive spectrometry (EDS) analysis was employed to determine the composition of CeO₂ (sample 8), nanoparticles (Figure 6). According to the obtained results which are reported in Table 5, the EDS clearly identify that the nanoparticles are composed of O and Ce, with the molar ratio of about 2:1 (O/Ce), they should therefore be attributed to CeO₂ and confirming the purity of nanoparticles.

The BET surface area of samples 1, 7 and 9 are reported in Table 6. The surface area increased by sonication time increasing, due to decrease of CeO₂ particle sizes. But, as the calcination temperature increases from 500 to 800°C, the surface area of CeO₂

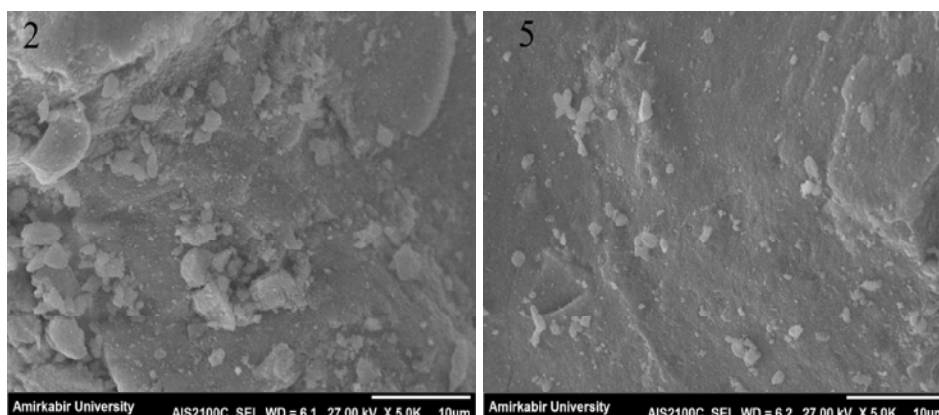


Fig. 4: SEM micrograph of synthesized CeO₂ at 5000X for 2 and 5 samples

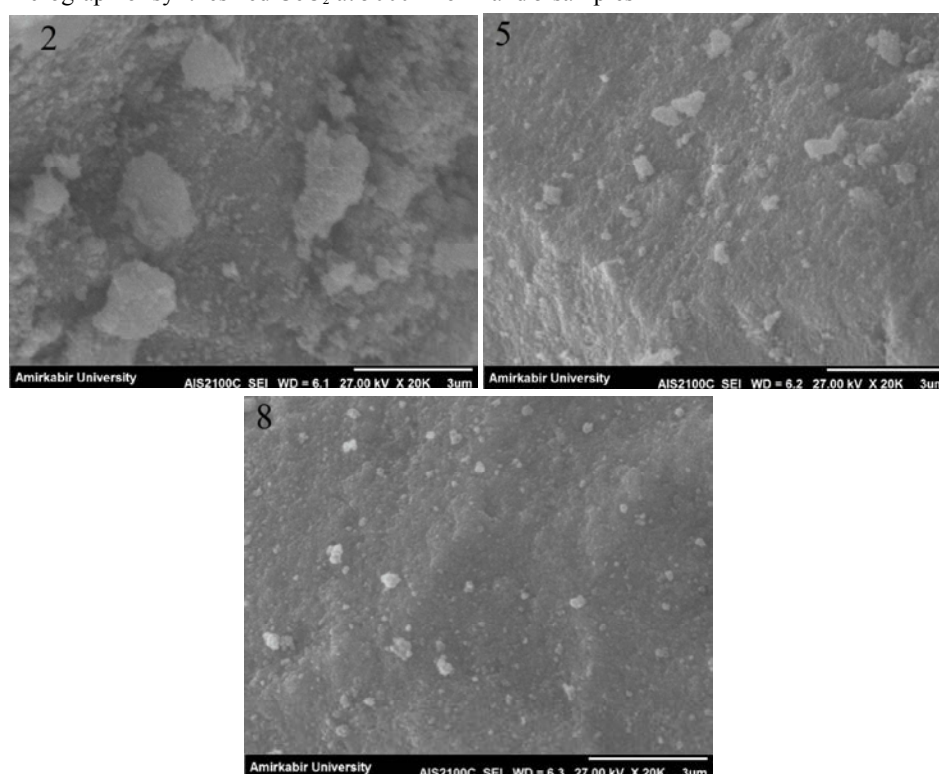


Fig. 5: SEM micrograph of synthesized CeO₂ at 20000X for 2, 5 and 8 samples

decreases due to the higher size of the formed particles and the subsequent loss of microporosity and increasing the pores volume on the surface of particles.

ESR Optimization for High H₂/CO: According to the design of experiments based on Taguchi method (Table 3), experiments 1-9 were performed. The analysis of the results (Table 7) carried out using QUALITEK-4 software. In Taguchi method the main effect of control factors indicates the trend of influence of a factor.

The results (Figures 7-10) indicate the average effects of sonication time, calcination temperature, H₂O/EtOH ratio and reactor temperature on H₂/CO values.

Another technique for optimization of the results suggested by Taguchi method is analysis of variance (ANOVA). This information displays relative influence of factor and interaction to the variation of results. The analysis of variance by QUALITEK-4 for this work is listed in Table 8. The numbers on the right hand side of the table indicate the “contribution” that a factor or

Table 5: EDS data obtained on sample 8

Element	W%	A%	Formula
O	16.46	64.25	-
Ce	72.09	32.12	CeO ₂
Au	11.45	3.63	Au
Total	100.00	100.00	-

Table 6: BET surface area

Sample no.	Surface area (m ² /g)
1	62.3
7	83.9
9	7.4

Table 7: The obtained experimental results

Experiment no.	X _{EIOH}	S _{H₂}	S _{CO}	H ₂ /CO
1	8.5	77.2	0.025	3082
2	5.6	52.2	0.338	154.5
3	5.5	48.9	0.012	4351
4	5.1	33.6	0.677	49.7
5	12.6	58.8	0.014	4129
6	2.0	73.5	0.017	3125
7	7.0	52.5	1.086	48.3
8	13.9	34.8	0.010	3374
9	1.6	44.0	0.012	3703

Table 8: Analysis of variance (ANOVA) for high H₂/CO values

Factors	DOF	Sum of squares	Variance	F-ratio	Pure sum	Percent
A	2	36319.3	18159.7	-	36319.3	0.14
B	2	10713927.6	5356963.8	-	10713927.6	40.43
C	2	6069583.5	3034791.8	-	6069583.5	22.91
D	2	9677200.0	4838600.0	-	4838600.0	36.52
Error	0	-	-	-	-	-
Total	8	26497030.4	-	-	-	100

Table 9: Modified ANOVA for for high H₂/CO

Factors	DOF	Sum of squares	Variance	F-ratio	Pure sum	Percent
A	0	-	-	-	-	0
B	2	10713927.6	5356963.8	295.0	10677608.3	40.30
C	2	6069583.5	3034791.8	167.1	6033264.2	22.77
D	2	9677200.0	4838600.0	266.5	9640880.6	36.38
Error	2	36319.3	18159.7	-	-	0.55
Total	8	26497030.4	-	-	-	100

Table 10: Optimum condition and estimate of performance at any arbitrary condition

Factor	Level description	Level	Contribution
A	pooled	-	-
B	800°C	3	1280.5
C	3	1	747.8
D	300°C	1	1190.8
Total contribution from all factors			3219.2
Current grand average of performance			2445.8
Expected result at optimum condition			5665.0

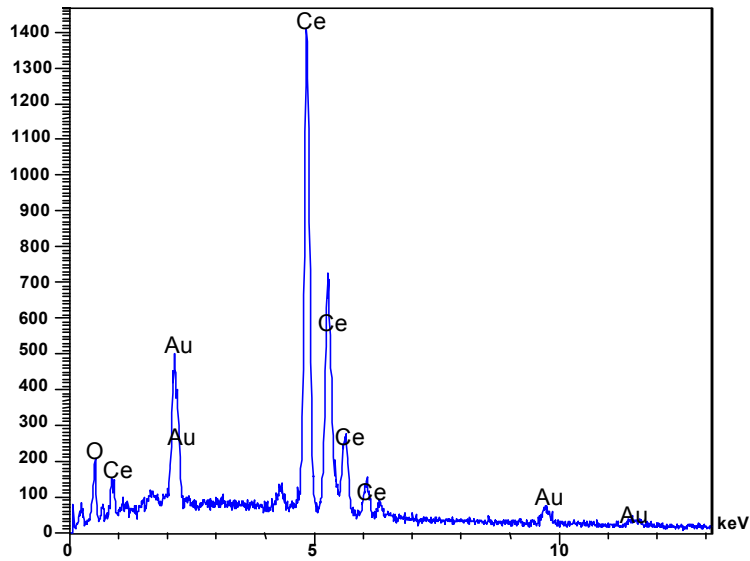


Fig. 6: EDS patterns of CeO₂ (sample 8)

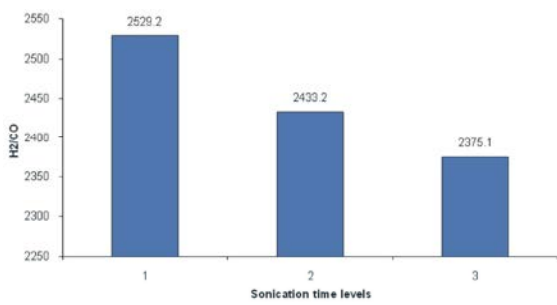


Fig. 7: Average effects of sonication time on H₂/CO values

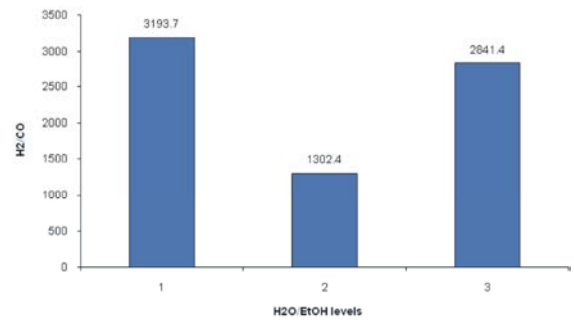


Fig. 9: Average effects of H₂O/EtOH on H₂/CO values

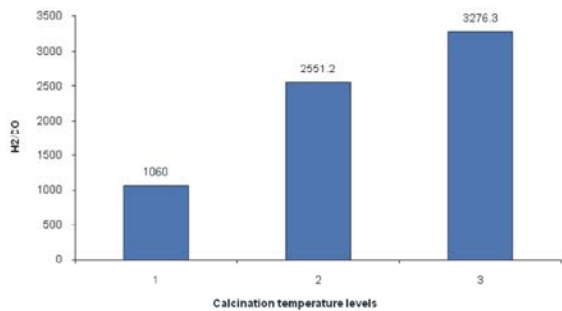


Fig. 8: Average effects of calcination temperature on H₂/CO values

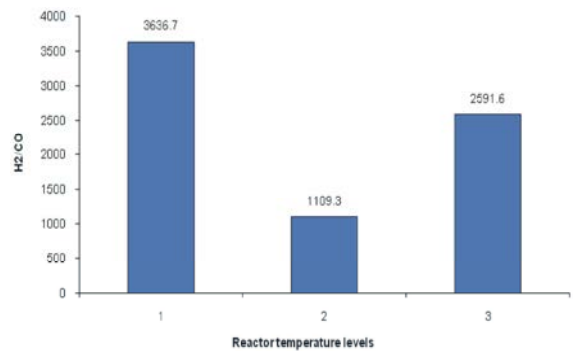


Fig. 10: Average effects of reactor temperature on H₂/CO values

interaction makes to the improvement of the expected performance. According to the results of Table 8, the factor that can be pooled and reach to the results of Table 9.

After ANOVA, the optimum conditions for the experiment can be reported. The QUALITEK-4 software calculates the performance at the optimum condition. Optimum conditions and best performance for our case

study are listed in Table 10. According to the Taguchi method, calcination temperature has the highest contribution in high H₂/CO ratio. The best setting for control factors are:

- Sonication time = 0 min
- Calcination temperature = 800°C
- H₂O/EtOH ratio = 3
- Reactor temperature = 300°C

Current grand average for H₂/CO ratio is around 2445. However at optimum conditions, the H₂/CO ratio is improved to around 5665. At the optimum conditions, the obtained results are:

- $S_{H_2} = 64.46$
- $S_{CO} = 0.011$
- H₂/CO = 5860

CONCLUSIONS

The effects of some different factors (sonication time, calcination temperature, Water/EtOH ratio and reactor temperature) on ceria (CeO₂) catalytic activity in ethanol steam reforming (ESR) to produce high H₂/CO ratio, were investigated. The Taguchi L₉ experimental design method was used to investigate the effect of these parameters on maximization of H₂/CO value. To identify the catalyst characteristics XRD, SEM, EDS, BET and TGA analysis were done. It was established that a face centered cubic crystal forms of nanoparticles of CeO₂ were formed. Also, by increasing calcination temperature or reducing the sonication time, the nanoparticle size was increased. The reactor tests showed that the optimum conditions for maximization of H₂/CO ratio are: sonication time zero, calcination temperature 800°C, H₂O/ethanol ratio 3 and reactor temperature 300°C. The mole percent of H₂ and CO in these conditions were 64.46% and 0.011%, respectively. According to the Taguchi method, calcination temperature has the highest contribution in maximization of H₂/CO ratio.

REFERENCES

1. Andrzej Denis, Wieslaw Grzegorzczak and Wojciech Gac andrzej Machocki, 2008. *Catalysis Today*, 137: 453-459.
2. Qi, A., B. Peppley and K. Karan, 2007. *Fuel Processing Technology*, 88: 3-22.
3. Haryanto, A., S. Fernando, N. Murali and S. Adhikari, 2008. *Energy Fuels*, 19: 2098-2106.
4. Bellido, J.D.A. and E.M. Assaf, 2008. *J. Power Sources*, 177: 24-32.
5. Tuti, S. and F. Pepe, 008. *Catal. Lett.*, 122: 196-203.
6. Profeti, L.P.R., E.A. Ticianelli and E.M. Assaf, 2008. *J. Power Sources*, 175: 482-489.
7. Vizcaino, A.J., A. Carriero and J.A. Calles, 2007. *Int. J. Hydrogen Energy*, 32: 1450-1461.
8. Koh, A.C.W., W.K. Leong, L. Chen, T.P. Ang, J. Lin, B.F.G. Johnson and T. Khimyak, 2008. *Catalysis Communications*, 9: 170-175.
9. Liguras, D.K., D. Kondarides and X.E. Verykios, 2003. *Appl. Catal. B*, 43: 345-354.
10. Montini, T., L. De Rogatis, V. Gombac, P. Fornasiero and M. Graziani, 2007. *Appl. Catal. B*, 71: 125-130.
11. Ni, M., D.Y.C. Leung and M.K.H. Leung, 2007. *Int. J. Hydrogen Energy*, 32: 3238-3247.
12. Zhang, B., X. Tang, Y. Li, W. Cai, Y. Xu and W. Shen, 2006. *Catalysis Communications*, 7: 367-372.
13. Diagne, C., H. Idriss and A. Kiennemann, 2002. *Catalysis Communications*, 3: 565-571.
14. Sun, J., Y. Wang, J. Li, G. Xiao, L. Zhang, H. Li, Y. Cheng, C. Sun, Z. Cheng, Z. Dong and L. Chen, 2010. *Int. J. Hydrogen Energy*, 35: 3087-3091.
15. Vasudeva, K., N. Mitra, P. Umasankar and S.C. Dhingra, 1996. *Int. J. Hydrogen Energy*, 21: 13-18.
16. Ioannides, T., 2001. *J. Power Sources*, 92: 17-25.
17. Luciene P.R. Profeti, Joelmir A.C. Dias, Jose M. Assaf and Elisabete M. Assaf, 2009. *J. Power Sources*, 190: 525-533.
18. Jalowiecki-Duhamel, L., C. Pirez, M. Capron, F. Dumeignil and E. Payen, 2010. *Catalysis Today*, 157: 456-461.
19. Park, S.H., 1996. *Robust design and Analysis for Quality Engineering*, Chapman & Hall, London.
20. Dipak Vitthal Pinjari, Aniruddha Bhalchandra Pandit, *Ultrasonics Sonochemistry*, 18: 1118-1123.
21. Chandramouleeswaran, S., S.T. Mhaske, A.A. Kathe, P.V. Varadarajan, V. Prasad and N. Vigneshwaran, *Nanotechnology*, 18: (art. no. 385702).
22. Zhang, Y., T. Cheng, O. Hu, Z. Fang and K. Han, 2007. *J. Mater. Res.*, 22: 1472-1478.
23. Higgins, S., N. Sammes and A. Smirnova, 2005. In *Proceedings of the 9th International Symposium on Solid Oxide Fuel Cells (SOFC-IX)*, May 2005, edited by J. Mizusaki, S.C. Singhal Electrochemical Society, pp: 1149.